

# Dynamic off-equilibrium transition in systems slowly driven across thermal first-order phase transitions

Andrea Pelissetto<sup>1</sup> and Ettore Vicari<sup>2</sup>

<sup>1</sup> *Dipartimento di Fisica di Sapienza, Università di Roma and INFN, Sezione di Roma I, I-00185 Roma, Italy and*

<sup>2</sup> *Dipartimento di Fisica dell'Università di Pisa and INFN, Largo Pontecorvo 3, I-56127 Pisa, Italy*

(Dated: June 5, 2021)

We study the off-equilibrium behavior of systems with short-range interactions, slowly driven across a thermal first-order transition, where the equilibrium dynamics is exponentially slow. We consider a dynamics that starts in the high- $T$  phase at time  $t = t_i < 0$  and ends at  $t = t_f > 0$  in the low- $T$  phase, with a time-dependent temperature  $T(t)/T_c \approx 1 - t/t_s$ , where  $t_s$  is the protocol time scale. A general off-equilibrium scaling (OS) behavior emerges in the limit of large  $t_s$ . We check it at the first-order transition of the two-dimensional  $q$ -state Potts model with  $q = 20$  and  $10$ . The numerical results show evidence of a dynamic transition, where the OS functions show a spinodal-like singularity. Therefore, the general mean-field picture valid for systems with long-range interactions is qualitatively recovered, provided the time dependence is appropriately (logarithmically) rescaled.

PACS numbers: 05.70.Fh, 05.70.Ln, 64.60.Ht, 05.50.+q

The dynamical behavior of statistical systems driven across phase transitions is a typical off-equilibrium phenomenon. Indeed, the large-scale modes present at the transition are unable to reach equilibrium as the system changes phase, even when the time scale  $t_s$  of the variation of the system parameters is very large. Such phenomena are of great interest in many different physical contexts [1–31]: One observes hysteresis and coarsening phenomena, the Kibble-Zurek defect production, etc. At continuous transitions, thermodynamic quantities obey general off-equilibrium scaling laws as a function of  $t_s$ , controlled by the universal static and dynamic exponents of the equilibrium transition [32, 33]. Similar results hold along the *magnetic* first-order transition line of systems with continuous  $O(N)$  symmetries ( $N > 1$ ) [34].

This Letter considers systems with short-range interactions undergoing a *thermal* first-order transition (FOT) driven by the temperature  $T$ . At the FOT temperature  $T_c$ , the energy density is discontinuous and any local dynamics is very slow, due to an exponentially large tunneling time between the two phases:  $\tau(L) \sim \exp(\sigma L^{d-1})$  for a system of size  $L^d$ , where the constant  $\sigma$  is related to the interface free energy. We study the off-equilibrium behavior arising when  $T$  is slowly varied across  $T_c \equiv \beta_c^{-1}$ . We consider a linear time dependence

$$\delta(t) \equiv \beta(t)/\beta_c - 1 = t/t_s, \quad \beta \equiv 1/T, \quad (1)$$

starting the dynamics at a time  $t_i < 0$  in the high- $T$  phase and ending it at  $t_f > 0$  in the low- $T$  phase.  $t_s$  is the time scale of the temperature variation. This protocol is general since a generic time dependence can be approximated by a linear function around  $T_c$ .

In the mean-field approximation, which becomes exact for long-range interactions [3], after crossing  $T_c$  the system persists in a metastable state with an infinite mean life, up to a spinodal-like point  $T_{sp} < T_c$ , thus up to a time  $t > 0$  such that  $\delta(t) = T_c/T_{sp} - 1$ , where a rapid

transition to the low- $T$  phase occurs. This picture requires a substantial revision in the case of short-range interactions, because metastable states may decay when  $T(t) < T_c$ , due to droplet formation [3].

We show that short-ranged systems at a thermal FOT show an off-equilibrium scaling (OS) behavior, which significantly differs from that obtained in the mean-field approximation. For finite  $t_s$  we observe a sharp transition to the low-temperature phase at a temperature  $T(t_s) < T_c$ , but the temperature  $T(t_s)$  approaches (logarithmically)  $T_c$  as  $t_s$  becomes large. Moreover, the time dependence of the OS functions develop a singular behavior characterized by peculiar scaling properties.

To test the general OS ideas, we consider the 2D Potts model, which is an ideal theoretical laboratory to study thermal FOTs. Its Hamiltonian reads

$$H = - \sum_{\langle \mathbf{x}\mathbf{y} \rangle} \delta(s_{\mathbf{x}}, s_{\mathbf{y}}), \quad (2)$$

where the sum is over the nearest-neighbor sites of a square lattice,  $s_{\mathbf{x}}$  (*color*) are integer variables  $1 \leq s_{\mathbf{x}} \leq q$ ,  $\delta(a, b) = 1$  if  $a = b$  and zero otherwise. It undergoes a phase transition [35, 36] at  $\beta_c = \ln(1 + \sqrt{q})$ , between a disordered phase and an ordered phase with  $q$  equivalent *vacua*. The transition is of first order for  $q > 4$ . We consider  $L \times L$  square lattices with periodic boundary conditions (PBC), which preserve the  $q$ -permutation symmetry. In infinite volume the energy density  $E = \langle H \rangle / L^2$  is discontinuous at  $T_c$ , with different [37]  $E_c^\pm \equiv E(T_c^\pm)$ . We define the *renormalized* energy density

$$E_r \equiv \Delta_e^{-1} (E - E_c^-), \quad \Delta_e \equiv E_c^+ - E_c^-, \quad (3)$$

which satisfies  $E_r = 0, 1$  for  $T \rightarrow T_c^-$  and  $T \rightarrow T_c^+$ , respectively. The magnetization

$$M_k = \frac{1}{L^2} \langle \sum_{\mathbf{x}} \mu_k(\mathbf{x}) \rangle, \quad \mu_k(\mathbf{x}) \equiv \frac{q\delta(s_{\mathbf{x}}, k) - 1}{q - 1}, \quad (4)$$

vanishes due to the  $q$ -state permutation symmetry, for any  $T$ . We consider the correlation function  $G_{kp}(\mathbf{x}, \mathbf{y}) \equiv \langle \mu_k(\mathbf{x}) \mu_p(\mathbf{y}) \rangle$ , and in particular its space integral

$$I_G = L^{-2} \sum_{k=1}^q \sum_{\mathbf{x}, \mathbf{y}} G_{kk}(\mathbf{x}, \mathbf{y}). \quad (5)$$

Equilibrium finite-size scaling (EFSS) holds also at FOTs [38–44]. For cubic-like lattices, the relevant scaling variable is  $r_1 = L^d \delta$ , where  $\delta \equiv \beta/\beta_c - 1$ . The energy density and  $I_G$  scale correspondingly as

$$E_r(T, L) \approx \mathcal{E}_{\text{eq}}(r_1), \quad I_G(T, L) \approx L^d \mathcal{C}_{\text{eq}}(r_1), \quad (6)$$

in the EFSS limit  $L \rightarrow \infty$  keeping  $r_1$  fixed. [45]

The system is driven across the transition by the temperature protocol (1), starting from equilibrated configurations at  $\beta = \beta_i = \beta(t_i) < \beta_c$ . Observables, such as  $E_r$  and  $I_G$ , are averaged at fixed  $t$  over the starting configurations. We anticipate that the OS behavior across the FOT does not depend on the value of  $\beta_i < \beta_c$ .

To specify the OS laws that describe the dynamic behavior for  $\beta(t) \approx \beta_c$ , we must identify the correct scaling variables. First, we use the variable  $r_1$ , parametrizing the EFSS functions, as equilibrium should be recovered in the appropriate limit. To define a second scaling variable, we should identify the appropriate time scale. When the global symmetry is preserved by the boundary conditions or in the absence of boundaries such as PBC, the the slowest mode in the system is the tunneling between the two phases. This is expected to proceed via mixed-phase strip-like configurations with two interfaces, whose probability is suppressed by a factor  $\exp(-\sigma L)$ , [46, 47] where  $\sigma = 2\beta_c \kappa$  and  $\kappa$  is the interface tension (which is exactly known for 2D Potts models [37]). Thus the relevant time is  $\tau(L) = L^\alpha \exp(\sigma L)$  where  $\alpha$  is an appropriate exponent. Therefore, the OS behavior is expected to be controlled by the scaling variables

$$r_1 = (t/t_s)L^2, \quad r_2 = t/\tau(L), \quad (7)$$

where  $t_s$  is the time scale of the protocol (1). The deviations from equilibrium are conveniently controlled by

$$s_1 = r_2/r_1 = t_s/[L^2\tau(L)]. \quad (8)$$

We expect  $E_r(t, t_s, L)$  and  $I_G(t, t_s, L)$ , defined as in Eqs. (3) and (5) and averaged at fixed  $t$ , to scale as

$$E_r \approx \mathcal{E}_s(s_1, r_1), \quad I_G \approx L^2 \mathcal{C}_s(s_1, r_1), \quad (9)$$

in the OS limit  $t, t_s, L \rightarrow \infty$  keeping  $r_1$  and  $s_1$  fixed, thereby extending the EFSS relations (6). EFSS should be recovered for  $s_1 \rightarrow \infty$ , where  $\mathcal{E}_s(s_1, r_1)$  and  $\mathcal{C}_s(s_1, r_1)$  converge to their equilibrium counterparts  $\mathcal{E}_{\text{eq}}(r_1)$  and  $\mathcal{C}_{\text{eq}}(r_1)$ . These OS arguments are quite general and can be extended to any thermal FOT, in any dimension [48].

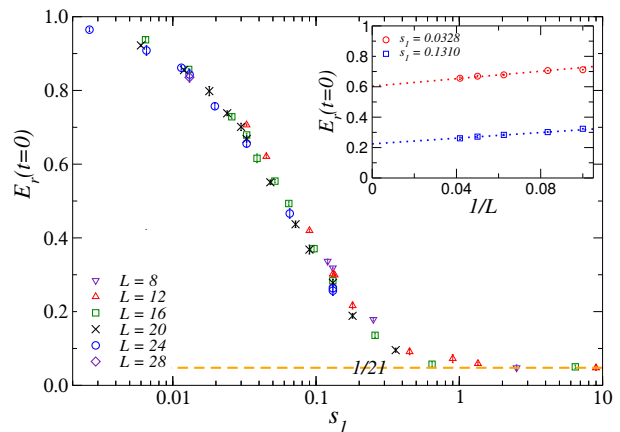


FIG. 1: (Color online) MC data of  $E_r$  for  $q = 20$  at  $t = 0$  versus  $s_1 = t_s/(L^{2+\alpha}e^{\sigma L})$ , using the optimal value  $\alpha = 2$  [50]. For  $s_1 \rightarrow \infty$ , the data converge to  $\mathcal{E}_{\text{eq}}(0) = 1/(1+q)$  (dashed line), since equilibrium is approached for  $t_s \gg \tau(L)$ . The inset shows the approach to the large- $L$  limit at fixed  $s_1$ .

The above OS theory is checked by a numerical analysis of Monte Carlo (MC) simulations of the 2D Potts model (2) for  $q = 20$  and  $q = 10$ . We mostly present results for  $q = 20$ . The dynamics is provided by the heat-bath algorithm [49], which is a representative of a purely relaxational dynamics. The time unit is a sweep of the whole lattice. The temperature is changed according to Eq. (1) every sweep, incrementing  $t$  by one.

We first consider data at  $t = 0$ , i.e.,  $r_1 = 0$ , as a function of  $s_1$ , see Fig. 1. Their optimal scaling is obtained when the power of the prefactor of  $\tau(L)$  is  $\alpha \approx 2$  [51]. We also verify the OS of  $E_r$  and  $I_G$  (and other observables) with respect to  $r_1$ , cf. Eq. (9), see [52]. Note that the approach to the OS curves requires the necessary condition  $L \gg \xi_{\pm}$  where  $\xi_{\pm}$  are the correlation lengths of the pure phases at  $T_c^{\pm}$  ( $\xi_- \approx \xi_+ = 2.695$  for  $q = 20$  [37]).

We now show that an interesting off-equilibrium behavior develops in the infinite-volume limit, corresponding to  $s_1 \rightarrow 0$ . As shown by Fig. 2, data at fixed  $t_s$  have a well-defined large- $L$  limit, see the inset of Fig. 2. This is rapidly approached for small values of  $\delta(t) \equiv t/t_s$ , e.g.,  $\delta(t) \lesssim 0.02$  at  $t_s \approx 10^5$ , while significantly larger lattices are required for larger  $\delta(t)$ . The energy density does not converge to its equilibrium value as  $L \rightarrow \infty$ , due to the fact that the system settles in a metastable state with large coexisting droplets of different colors.

The infinite-volume energy density (see Fig. 2) takes the equilibrium high- $T$  value  $E_r(t=0) = 1$  at  $t = 0$  for any  $t_s$ , then shows a sharp decrease at a point  $\delta^*(t_s)$ , which decreases with increasing  $t_s$ . The system develops a nontrivial OS behavior close to  $\delta^*(t_s)$ . For large  $L$  the system behaves as a gas of droplets of size  $R$  (evidence for this behavior is provided in [52]). The relevant scaling variables are expected to be analogous to  $r_1$  and  $r_2$ , cf. Eq. (7), with  $R$  replacing the size  $L$ . The relevant

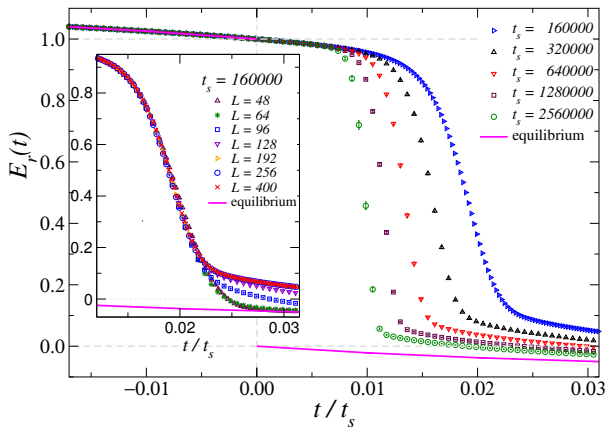


FIG. 2: (Color online) MC data of  $E_r(t)$  for  $q = 20$  for some values of  $t_s$ , in the  $L \rightarrow \infty$  limit. The large- $L$  convergence (within errors) is checked by increasing  $L$  at fixed  $t_s$ , analogously to the case shown in the inset. The full lines show the equilibrium energy density at  $\beta = \beta_c(1 + t/t_s)$ .

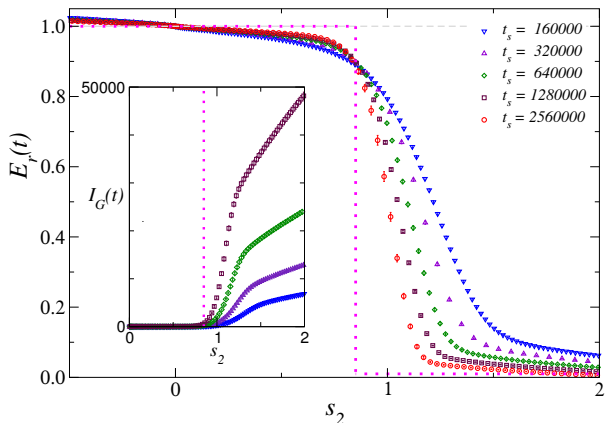


FIG. 3: (Color online) The infinite-volume  $E_r$  and  $I_G$  (inset) for  $q = 20$  versus  $s_2$ . The dotted lines show the conjectured singular large- $t_s$  limit, see text.

time scale is that of the formation of droplets of size  $R$ . As the time  $\tau_d$  to create a droplet of size  $R$  increases exponentially with  $R$ ,  $\ln \tau_d \sim R$ , we expect  $R \sim \ln t$ . Thus, the analogue of the scaling variable  $r_1$  becomes ( $t > 0$ )

$$s_2 = (t/t_s) \ln^2 t. \quad (10)$$

In Fig. 3 we report the infinite-volume energy density and  $I_G$  for  $q = 20$  versus  $s_2$ . We note a crossing point of the energy curves for different values of  $t_s$  at approximately  $s_2^* \approx 0.85$  with  $E_r^* \approx 0.89$ . At the same value of  $s_2$ ,  $I_G$  shows a sharp change of behavior. These results suggest that, in the limit  $t_s \rightarrow \infty$ , the OS functions develop a singular behavior for  $s_2 = s_2^*$ . In particular, the infinite-volume energy density takes the high- $T$  value  $\mathcal{E}_\infty(s_2) = e_+ = 1$  for  $s_2 < s_2^*$ , while we expect  $\mathcal{E}_\infty(s_2) = e_- \ll 1$  for  $s_2 > s_2^*$ . Note that, for large  $t_s$ ,  $(t \ln^2 t)/t_s = s_2^*$  implies  $t/t_s \approx s_2^*/(\ln t_s)^2$ , so that the value  $\beta_d$  of  $\beta$  at which the

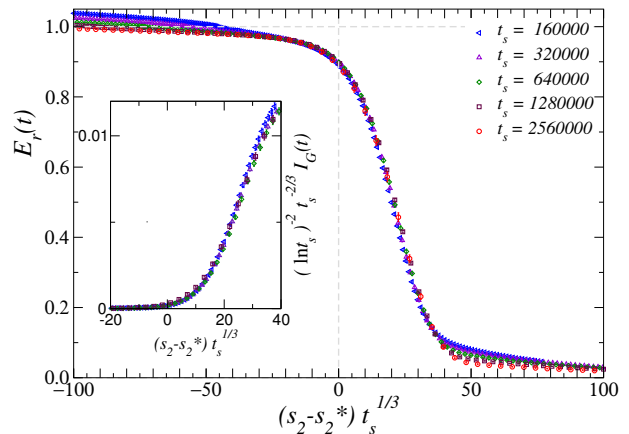


FIG. 4: (Color online) Scaling of the infinite-volume  $E_r$  and  $I_G$  (inset) around  $s_2^*$ .

sharp change occurs converges to  $\beta_c$  as  $t_s$  increases.

The behavior around  $s_2^*$  turns out to be described by an additional scaling Ansatz. As shown in Fig. 4, the energy density  $\mathcal{E}_\infty(s_2, t_s) \equiv E_r(t, t_s, L \rightarrow \infty)$  scales as

$$\mathcal{E}_\infty(s_2, t_s) \approx f_e(\tilde{s}_2), \quad \tilde{s}_2 = (s_2 - s_2^*) t_s^\theta \quad (11)$$

with [51]  $\theta = 1/3$ . We stress that scaling is only observed when using the variable  $s_2$ . The estimate  $\theta = 1/3$  is reasonably accurate (10% accuracy). Also  $I_G(s_2, t_s)$  shows a scaling behavior, provided we multiply it by an additional power of  $t_s$ . Phenomenologically we observe  $I_G(t) \approx (\ln t_s)^2 t_s^{2/3} f_G(\tilde{s}_2)$ , see the inset of Fig. 4 (the exponents of  $t_s$  and  $\ln t_s$  in the prefactor are an educated guess). A similar analysis can be performed for  $q = 10$ , see [52]. The estimate of  $s_2^*$  changes ( $s_2^* \approx 0.2$  for  $q = 10$ ), but all other conclusions hold. In particular, MC data are again consistent with  $\theta = 1/3$ . This singular behavior resembles that at the mean-field spinodal point [3], or more generally the power-law scaling at equilibrium continuous transitions. However, here the location  $\beta_d$  of the dynamic transition converges to  $\beta_c$  as  $t_s \rightarrow \infty$ :  $\beta_d - \beta_c \sim (\ln t_s)^{-2} \rightarrow 0$  [58].

To understand the behavior of the system for  $s_2 \approx s_2^*$ , one may consider the evolution of the size of the clusters formed by spins of the same color. A typical case is reported in Fig. 5. For  $s_2 \lesssim s_2^*$ , the system is disordered and all clusters are small: their typical size  $\ell_d$  satisfies  $\ell_d \lesssim \xi_+$ , where  $\xi_+$  is the correlation length of the pure disordered phase [37]. For  $s_2 \approx s_2^*$  clusters start growing. There is a short coarsening interval [5, 8, 33], in which  $E_r$  decreases almost linearly. Then, the system settles in a metastable state characterized by many coexisting large clusters. Details are reported in [52].

One may also consider the dynamics induced by the reverse linear protocol across  $\beta_c$ , starting from an ordered configuration (equal spins) at  $\beta_i > \beta_c$  and decreasing  $\beta$  across the FOT,  $\beta(t) = \beta_c(1 - t/t_s)$ , up to  $\beta_f < \beta_c$ .

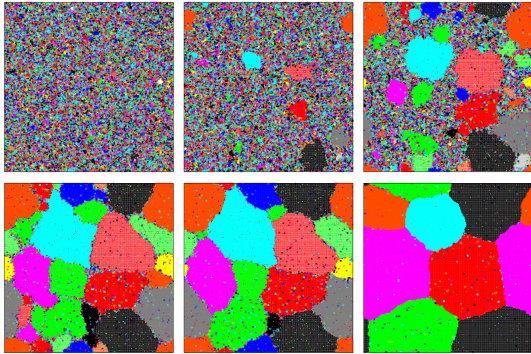


FIG. 5: (Color online) Snapshots of a system of size  $L = 512$  for  $\tilde{s}_2 = (s_2 - s_2^*)t_s^{1/3} = -20, 0, 20, 40, 100, 1500$ , (from left to right, top to bottom). Here  $q = 20$  and  $t_s = 640000$ . We use different colors for each value of  $s_x$ . The range of  $\tilde{s}_2$  covers the region where  $E_r$  significantly changes, see Fig. 4.

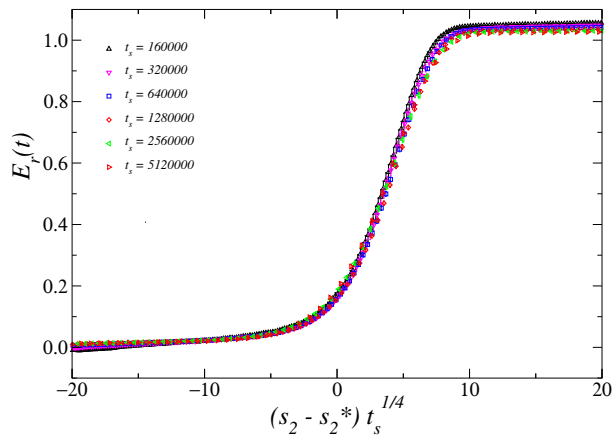


FIG. 6: (Color online) Scaling of the infinite-volume  $E_r$  for the reversed protocol, in which the dynamics starts from an ordered configuration at  $\beta_i > \beta_c$  and  $\beta(t) = \beta_c(1 - t/t_s)$ . The optimal collapse is obtained for  $s_2^* \approx 0.85$  and  $\theta \approx 1/4$  [the accuracy of the data does not exclude the value  $\theta \approx 1/3$  obtained for protocol (1)], see [52].

In this case the  $q$ -permutation symmetry is broken by the initial condition. MC results show an analogous OS behavior. In the infinite-volume limit the system persists in the ordered state up to a temperature  $T(t_s) > T_c$ , where it transits to the disordered state. For  $T \approx T(t_s)$  one observes analogous OS laws. Eq. (11) holds with a corresponding  $s_2^*$  and exponent  $\theta$ , which may differ from those of protocol (1), see Fig. 6 and [52].

The OS theory can be applied to hysteresis phenomena that occur when  $T$  is first decreased below  $T_c$  and then increased above  $T_c$ . We mention that external periodically-varying fields have been already considered at magnetic FOTs, where they give rise to a singular dynamic behav-

ior of the magnetization hysteresis [59, 60].

In conclusion, we have developed an OS theory to describe the off-equilibrium behavior of statistical systems when their temperature is slowly varied across a thermal FOT. We consider the linear protocol (1) and the reversed one [61]. Our numerical study of the Potts model confirms the general OS theory. In particular, in the infinite-volume limit it shows two dynamic regimes, separated by a spinodal-like transition point where the OS functions are singular. Such a transition occurs at a time  $t_d > 0$  scaling as  $t_d \sim t_s(\ln t_s)^{-2}$  in the large- $t_s$  limit. Therefore, a spinodal-like behavior emerges dynamically in short-range models, without assuming long-range interactions as in the mean-field theory [3]. The OS behavior arises from the interplay between the exponentially large tunneling times at  $T_c$  and the droplet formation. We expect that analogous dynamic scalings emerge at any thermal FOT characterized by these two features. Further investigations are needed to clarify its degree of universality and to develop a theory which is able to predict the exponent  $\theta$  entering the OS laws, such as Eq. (11).

Our results provide an effective framework to interpret experimental data in many physical contexts, when thermal FOTs are crossed by slowly varying  $T$ . For example, we mention the formation of the quark-gluon plasma in heavy-ion collisions [62], whose intrinsic space-time inhomogeneities complicate the study of the hadronic phase diagram, and, in particular, the expected thermal FOT line at nonzero baryon chemical potential [63]. Another issue concerns the universe evolution. Kibble [1] made the first analysis of the behavior of a system going across a continuous transition, to study the defect production during the universe expansion. Analogous studies at FOTs may shed some light on the behavior of an expanding and cooling universe going across a FOT [64].

- 
- [1] T. W. B. Kibble, Topology of cosmic domains and strings, *J. Phys. A* **9**, 1387 (1976).
  - [2] W. H. Zurek, Cosmological experiments in superfluid helium?, *Nature* **317**, 505 (1985).
  - [3] K. Binder, Theory of first-order phase transitions, *Rep. Prog. Phys.* **50**, 783 (1987).
  - [4] A. Polkovnikov, K. Sengupta, A. Silva, and M. Vengalattore, Colloquium: Nonequilibrium dynamics of closed interacting quantum systems, *Rev. Mod. Phys.* **83**, 863 (2011).
  - [5] G. Biroli, Slow Relaxations and Non-Equilibrium Dynamics in Classical and Quantum Systems, arXiv:1507.05858.
  - [6] I. Chuang, R. Durrer, N. Turok, and B. Yurke, Cosmology in the Laboratory: Defect Dynamics in Liquid Crystals, *Science* **251**, 1336 (1991).
  - [7] M. J. Bowick, L. Chandar, E. A. Schiff, and A. M. Srivastava, The Cosmological Kibble Mechanism in the Labora-

- tory: String Formation in Liquid Crystals, *Science* **263**, 943 (1994).
- [8] A.J. Bray, Theory of phase-ordering kinetics, *Adv. Phys.* **43**, 357 (1994).
- [9] C. Bäuerle, Yu M. Bunkov, S. N. Fisher, H. Godfrin, and G. R. Pickett, Laboratory simulation of cosmic string formation in the early Universe using superfluid  $^3\text{He}$ , *Nature* **382**, 332 (1996).
- [10] V. M. H. Ruutu, V. B. Eltsov, A. J. Gill, T. W. B. Kibble, M. Krusius, Y. G. Makhlin, B. Placais, G. E. Volovik, and W. Xu, Vortex formation in neutron-irradiated superfluid  $^3\text{He}$  as an analogue of cosmological defect formation, *Nature* **382**, 334 (1996).
- [11] R. Carmi, E. Polturak, and G. Koren, Observation of Spontaneous Flux Generation in a Multi-Josephson-Junction Loop, *Phys. Rev. Lett.* **84**, 4966 (2000).
- [12] S. Casado, W. González-Viñas, H. Mancini, and S. Boccaletti, Topological defects after a quench in a Benard-Marangoni convection system, *Phys. Rev. E* **63**, 057301 (2001).
- [13] R. Monaco, J. Mygind, and R. J. Rivers, Observation of Spontaneous Flux Generation in a Multi-Josephson-Junction Loop, *Phys. Rev. Lett.* **89**, 080603 (2002).
- [14] A. Maniv, E. Polturak, and G. Koren, Observation of Magnetic Flux Generated Spontaneously During a Rapid Quench of Superconducting Films, *Phys. Rev. Lett.* **91**, 197001 (2003).
- [15] P. Calabrese and A. Gambassi, Ageing Properties of Critical Systems, *J. Phys. A* **38**, R133 (2005).
- [16] S. Casado, W. González-Viñas, and H. Mancini, Observation of Magnetic Flux Generated Spontaneously During a Rapid Quench of Superconducting Films, *Phys. Rev. E* **74**, 047101 (2006).
- [17] R. Monaco, J. Mygind, M. Aaroe, R. J. Rivers, and V.P. Koshelets, Zurek-Kibble Mechanism for the Spontaneous Vortex Formation in NbAl/AlOx/Nb Josephson Tunnel Junctions: New Theory and Experiment, *Phys. Rev. Lett.* **96**, 180604 (2006).
- [18] L.E. Sadler, J.M.Higbie, S.R. Leslie, M. Vengalattore, and D.M. Stamper-Kurn, Spontaneous symmetry breaking in a quenched ferromagnetic spinor Bose-Einstein condensate, *Nature* **443**, 312 (2006).
- [19] C.N. Weiler, T. W. Neely, D. R. Scherer, A. S. Bradley, M. J. Davis and B. P. Anderson, Spontaneous vortices in the formation of Bose-Einstein condensates, *Nature* **455**, 948 (2008).
- [20] D. Golubchik, E. Polturak, and G. Koren, Evidence for Long-Range Correlations within Arrays of Spontaneously Created Magnetic Vortices in a Nb Thin-Film Superconductor, *Phys. Rev. Lett.* **104**, 247002 (2010).
- [21] D. Chen, M. White, C. Borries, and B. DeMarco, Quantum Quench of an Atomic Mott Insulator, *Phys. Rev. Lett.* **106**, 235304 (2011).
- [22] S. C. Chae, N. Lee, Y. Horibe, M. Tanimura, S. Mori, B. Gao, S. Carr, and S.-W. Cheong Direct Observation of the Proliferation of Ferroelectric Loop Domains and Vortex-Antivortex Pairs, *Phys. Rev. Lett.* **108**, 167603 (2012).
- [23] M.A. Miranda, J. Burguete, H. Mancini, and W. González-Viñas, Frozen dynamics and synchronization through a secondary symmetry-breaking bifurcation, *Phys. Rev. E* **87**, 032902 (2013).
- [24] S. Ejtemaee and P. C. Haljan, Spontaneous nucleation and dynamics of kink defects in zigzag arrays of trapped ions, *Phys. Rev. A* **87**, 051401(R) (2013).
- [25] S. Ulm, S. J. Ronagel, G. Jacob, C. Degen, S. T. Dawkins, U. G. Poschinger, R. Nigmatullin, A. Retzker, M. B. Plenio, F. Schmidt-Kaler, and K. Singer, Observation of the Kibble-Zurek scaling law for defect formation in ion crystals, *Nat. Commun.* **4**, 2290 (2013).
- [26] K. Pyka, J. Keller, H. L. Partner, R. Nigmatullin, T. Burgermeister, D. M. Meier, K. Kuhlmann, A. Retzker, M. B. Plenio, W. H. Zurek, A. del Campo, and T. E. Mehlstäubler, Topological defect formation and spontaneous symmetry breaking in ion Coulomb crystals, *Nat. Commun.* **4**, 2291 (2013).
- [27] G. Lamporesi, S. Donadello, S. Serafini, F. Dalfovo, and G. Ferrari, Spontaneous creation of Kibble-Zurek solitons in a Bose-Einstein condensate, *Nat. Phys.* **9**, 656 (2013).
- [28] L. Corman, L. Chomaz, T. Bienaimé, R. Desbuquois, C. Weitenberg, S. Nascimbene, J. Dalibard, and J. Beugnon, Quench-Induced Supercurrents in an Annular Bose Gas, *Phys. Rev. Lett.* **113**, 135302 (2014).
- [29] N. Navon, A. L. Gaunt, R. P. Smith, and Z. Hadzibabic, Critical Dynamics of Spontaneous Symmetry Breaking in a Homogeneous Bose gas, *Science* **347**, 167 (2015).
- [30] S. Braun, M. Friesdorf, S.S. Hodgman, M. Schreiber, J.P. Ronzheimer, A. Riera, M. del Rey, I. Bloch, J. Eisert, and U. Schneider, Emergence of coherence and the dynamics of quantum phase transitions, *PNAS* **112**, 3641 (2015).
- [31] M. J. Davis, T. M. Wright, T. Gasenzer, S. A. Gardiner, and N. P. Proukakis, Formation of Bose-Einstein condensates, arXiv:1601.06197.
- [32] S. Gong, F. Zhong, X. Huang, and S. Fan, Finite-time scaling via linear driving, *New J. Phys.* **12**, 043036 (2010).
- [33] A. Chandran, A. Erez, S. S. Gubser, and S. L. Sondhi, Kibble-Zurek problem: Universality and the scaling limit, *Phys. Rev. B* **86**, 064304 (2012).
- [34] A. Pelissetto and E. Vicari, Off-equilibrium scaling behaviors driven by time-dependent external fields in three-dimensional  $O(N)$  vector models, *Phys. Rev. E* **93**, 032141 (2016).
- [35] R.J. Baxter, *Exactly solved models in statistical mechanics*, (Academic Press, 1982).
- [36] Several exact results are reported in F.Y. Wu, The Potts model, *Rev. Mod. Phys.* **54**, 235 (1982).
- [37] At the FOT for  $q = 20$ :  $E(T_c^+) = -0.626530\dots$ ,  $E(T_c^-) = -1.820584\dots$ ,  $\beta_c\kappa = 0.185494\dots$  gives the interface tension [53], the magnetization  $m_c = \lim_{T \rightarrow T_c^-} \lim_{h_k \rightarrow 0} \lim_{V \rightarrow \infty} M_k = 0.941175\dots$  where  $h_k$  is a *magnetic* field, the correlation length  $\xi_+ = 2.6955\dots$  for  $T \rightarrow T_c^+$ . [35, 36, 53–55]
- [38] B. Nienhuis and M. Nauenberg, First-Order Phase Transitions in Renormalization-Group Theory, *Phys. Rev. Lett.* **35**, 477 (1975).
- [39] M.E. Fisher and A.N. Berker, Scaling for first-order phase transitions in thermodynamic and finite systems, *Phys. Rev. B* **26**, 2507 (1982).
- [40] V. Privman and M. E. Fisher, Finite-size effects at first-order transitions, *J. Stat. Phys.* **33**, 385 (1983).
- [41] M. E. Fisher and V. Privman, First-order transitions breaking  $O(n)$  symmetry: Finite-size scaling, *Phys. Rev. B* **32**, 447 (1985).
- [42] M.S.S. Challa, D.P. Landau, and K. Binder, Finite-size effects at temperature-driven first-order transitions, *Phys. Rev. B* **34**, 1841 (1986).

- [43] C. Borgs and R. Kotecky, A rigorous theory of finite-size scaling at first-order phase transitions, *J. Stat. Phys.* **61**, 79 (1990).
- [44] M. Campostrini, J. Nespolo, A. Pelissetto, and E. Vicari, Finite-size scaling at first-order quantum transitions, *Phys. Rev. Lett.* **113**, 070402 (2014); Finite-size scaling at first-order quantum transitions of quantum Potts chains, *Phys. Rev. E* **91**, 052103 (2015).
- [45] For example, in the case of the  $q$ -state Potts model with PBC, the EFSS limit of the energy density is  $\mathcal{E}_{\text{eq}}(r_1) = (1 + q e^X)^{-1}$  with  $X = \Delta_e \beta_c L^2 \delta = \Delta_e \beta_c r_1$ . See [52] for details.
- [46] B. A. Berg and T. Neuhaus, Multicanonical ensemble: A new approach to simulate first-order phase transitions, *Phys. Rev. Lett.* **68**, 9 (1992).
- [47] Non-symmetric boundary conditions inducing the presence of an interface are considered in H. Panagopoulos and E. Vicari, Off-equilibrium scaling across a first-order transition, *Phys. Rev. E* **92**, 062107 (2015). In these cases the dynamics at the FOT is characterized by a time scale increasing as a power of the size, i.e.,  $\tau(L) \sim L^3$ .
- [48] In  $d$  dimensions,  $r_1 = (t/t_s)L^d$ ,  $r_2 = t/\tau(L)$  with  $\tau(L) = L^\alpha \exp(\sigma L^{d-1})$ , and  $s_1 = t_s/[L^d \tau(L)]$ .
- [49] A heat-bath updating of a single site variable consists in the change  $s_{\mathbf{x}} \rightarrow s'_{\mathbf{x}}$  with probability  $\sim e^{-H(s'_{\mathbf{x}})/T}$  independent of the original spin  $s_{\mathbf{x}}$ .
- [50] This is obtained by an educated guess after looking at the data. Unbiased analyses confirm it with 20% accuracy. We note that the precision on the exponent  $\alpha$  of the prefactor of  $\tau(L) = L^\alpha e^{\sigma L}$  is not crucial for the scaling behavior, which is essentially controlled by the dominant exponential dependence.
- [51] We are biased by the idea that simple integer or fractional exponents enter the various off-equilibrium scaling ansatzs at FOTs, likely arising from geometric reasons.
- [52] See Supplementary Material associated with this paper, where we report some additional results for the OS behavior in finite and infinite volume, for linear protocols from the high- $T$  to the low- $T$  phase and viceversa, and includes Refs. [35, 36, 42, 43, 53–57].
- [53] A. Billoire, T. Neuhaus, B. A. Berg, A determination of interface free energies, *Nucl. Phys. B* **413**, 795 (1994).
- [54] C. Borgs and W. Janke, An explicit formula for the interface tension of the 2D Potts model, *J Phys. I (France)* **2**, 2011 (1992).
- [55] A. Tröster and K. Binder, Microcanonical determination of the interface tension of flat and curved interfaces from Monte Carlo simulations, *J. Phys.: Condens. Matter* **24**, 284107 (2012).
- [56] F. Igloi and E. Carlon, Boundary and bulk phase transitions in the two-dimensional  $Q$ -state Potts model ( $Q > 4$ ), *Phys. Rev. B* **59**, 3783 (1999).
- [57] W. Janke and S. Kappler, 2D Potts-Model Correlation Lengths: Numerical Evidence for  $\xi_o = \xi_d$  at  $\beta_t$ , *Europhys. Lett.* **31**, 345 (1995).
- [58] Similar results are obtained under different dynamical conditions, see, e.g., J. L. Meunier and A. Morel, Condensation and metastability in the 2D Potts model, *Eur. Phys. J B* **13**, 341 (2000); E. S. Loscar, E. E. Ferrero, T. S. Grigera, and S. A. Cannas, Nonequilibrium characterization of spinodal points using short time dynamics, *J. Chem. Phys.* **131**, 024120 (2009); T. Nogawa, N. Ito, and H. Watanabe, Static and dynamical aspects of the metastable states of first order transition systems, *Physics Procedia* **15**, 76 (2011); M. Ibàñez Berganza, P. Coletti and A. Petri, Anomalous metastability in a temperature-driven transition, *Europhys. Lett.* **106**, 56001 (2014).
- [59] B. Chakrabarti and M. Acharyya, Dynamic transitions and hysteresis, *Rev. Mod. Phys.* **71**, 847 (1999).
- [60] S. W. Sides, P. A. Rikvold, and M. A. Novotny, Kinetic Ising Model in an Oscillating Field: Finite-Size Scaling at the Dynamic Phase Transition, *Phys. Rev. Lett.* **81**, 834 (1998); G. Korniss, P. A. Rikvold, and M. A. Novotny, Absence of first-order transition and tricritical point in the dynamic phase diagram of a spatially extended bistable system in an oscillating field, *Phys. Rev. E* **66**, 056127 (2002).
- [61] Linear time variations are quite general since any generic time dependence can be linearly approximated around  $T_c$ . If the linear term is present, higher-order contributions are suppressed in the OS limit (this can be shown by scaling arguments); if it is absent, the OS behavior changes, but it can still be derived by a generalization of the scaling arguments.
- [62] J.D. Bjorken, Highly relativistic nucleus-nucleus collisions: The central rapidity region, *Phys. Rev. D* **27**, 140 (1983).
- [63] K. Rajagopal and F. Wilczek, in *At the Frontier of Particle Physics / Handbook of QCD*, M. Shifman, ed., (World Scientific, 2001); arXiv:hep-ph/0011333.
- [64] D. Boyanovsky, J. J. de Vega, and D. J. Schwarz, Phase transitions in the early and the present universe, *Ann. Rev. Nucl. Part. Sci.* **56**, 441 (2006).